Supramolecular Chemistry
Publication details, including instructions for authors and subscription information:
http://www.informaworld.com/smpp/title~content=t713649759

Preparation of Pyridinium Iodide-CdI_2 Hybrids for Nonlinear Optical Materials

Hiroaki Kosuge[a]; Shuji Okada[a]; Hidetoshi Oikawa[a]; Hachiro Nakanishi[a]
[a] Institute for Chemical Reaction Science, Tohoku University, Sendai, Japan

To cite this Article Kosuge, Hiroaki , Okada, Shuji , Oikawa, Hidetoshi and Nakanishi, Hachiro(2001) 'Preparation of Pyridinium Iodide-CdI_2 Hybrids for Nonlinear Optical Materials', Supramolecular Chemistry, 13: 1, 233 — 245
To link to this Article: DOI: 10.1080/10610270108034896
URL: http://dx.doi.org/10.1080/10610270108034896

SUPRAMOLECULAR CHEMISTRY, Vol. 13, pp. 233-245
Reprints available directly from the publisher
Photocopying permitted by license only

Preparation of Pyridinium Iodide-CdI_2 Hybrids for Nonlinear Optical Materials

HIROAKI KOSUGE, SHUJI OKADA, HIDETOSHI OIKAWA
and HACHIRO NAKANISHI*

Institute for Chemical Reaction Science, Tohoku University, Sendai 980-8577, Japan

In order to obtain a new type of organic-inorganic hybrid material for nonlinear optics, two pyridinium-CdI_2 crystals, *i.e.*, *bis*(4-cyano-1-methylpyridinium) tetraiodocadmate (CNP/CdI_4) and *bis*(4-dimethylamino-1-methylpyridinium) tetraiodocadmeate (DAP/CdI_4) were prepared. From X-ray crystal structure analyses, the inorganic parts of both of the crystals are found to be the tetrahedral $[CdI_4]^{2-}$ structure. Although the CNP/CdI_4 crystals have a centrosymmetric layered structure, the DAP/CdI_4 crystals do not have layered structures resulting in non-centrosymmetric space group *Cc* and second-order nonlinear optical activity. Thus, the second-harmonic generation (SHG) coefficients (*d*) of the DAP/CdI_4 crystal were estimated using the oriented gas model. In spite of the shorter cutoff wavelength of DAP/CdI_4 compared with that of the well-known 2-methyl-4-nitroaniline (MNA) crystal, the maximum *d* value was expected to reach one-third of that of the MNA in the diagonal component.

Keywords: Organic-inorganic hybrid crystal; Structure analysis; Nonlinear optical material; Second-harmonic generation

INTRODUCTION

In the past two decades, many organic crystals have been designed and synthesized for second-order nonlinear optical (NLO) materials [1-6]. The requirements for second-order organic NLO crystals have been well established as follows: First, molecules in the materials should have large hyperpolarizability (β). Secondly, these molecules should be aligned, at least in non-centrosymmetric crystal structures and hopefully in optimal orientation to maximize NLO properties in bulk. The absorption of the materials should not be at the laser wavelengths concerned. Crystal growing ability is also an important factor. Although further processability of single crystals is also indispensable for device fabrication, many organic crystals are too fragile to cut and polish because conventional organic molecules are assembled only by a weak attractive force like the van der Waals force. However, in the case of organic ionic crystals, mechanical properties can be improved due to strong Coulombic interactions. One of the examples of organic ionic NLO crystals is 1-methyl-4-(2-(4-(dimethylamino)phenyl)ethenyl-pyridinium *p*-toluenesufonate (DAST) [7-9]. In this compound, the β value of the cationic species for molecular long-axis direction was found to be very large compared with that of non-ionic species with similar π-conjugation lengths [10]. This fact and proper alignment of

---

*Corresponding author.

the ionic species result in a large second-harmonic generation (SHG) coefficient (*d*) and electro-optic (EO) coefficient (*r*) among organic compounds [11, 12].

Since organic ionic crystals have several advantages as mentioned above, extended studies on organic ionic crystals seemed to be worth investigating. In this study, we prepared hybrid crystals composed of pyridinium cations and divalent metal halide. 4-Substituted pyridinium cations, as shorter π-conjugated systems of the DAST cation, were found to have comparatively large β in spite of no absorption in the visible region [13], and several crystals with benzenesulfonate derivatives as counter anions were prepared for frequency conversion of diode lasers [14–16]. It is well known that the combination of primary ammonium halide ($RNH_3^+X^-$) and divalent metal halide (MX_2) gives a layered perovskite structure in the general formula of $(RNH_3)_2MX_4$, which shows interesting optical properties [17–21]. However, combination with pyridinium halides has not been studied so far. This paper concerns with two hybrid crystals prepared from 4-substituted pyridinium iodide and cadmium iodide. The crystal structures and the estimated *d* value of the crystal with a non-centrosymmetric structure are reported.

RESULTS AND DISCUSSION

Two kinds of hybrid crystals were prepared by simple mixing of substituted pyridinium iodide ethanol solution and cadmium iodide ethanol solution in a molar ratio of 2 : 1. Pyridinium derivatives used were 4-cyano-1-methylpyridinium (CNP) and 4-dimethylamino-1-methylpyridinium (DAP). From elementary analysis of the precipitated crystals by solution mixing, composition of the hybrid crystals was confirmed to be 2 : 1 complexes between pyridinium iodide and cadmium iodide (Fig. 1) [22]. Melting points of these crystals were found to be 220°C for bis(4-cyano-1-methylpyridinium) tetraiodocadmate (CNP/CdI_4) and 172°C for bis(4-dimethylamino-1-methylpyridinium) tetraiodocadmeate (DAP/CdI_4), respectively. CNP/CdI_4 has a higher melting point than CNP iodide (200°C), whereas DAP/CdI_4 has a lower melting point than DAP iodide (250°C). Although CNP/CdI_4 decomposed above its melting point, DAP/CdI_4 did not decompose at all in the molten state until 300°C. These behaviors were similar to their iodide salts: CNP iodide decomposed above its melting point, while DAP iodide did not decompose until 300°C. It seemed that the stability of hybrid compounds is mainly limited by the stability of organic cation parts. High stability of DAP/CdI_4 in the molten state may allow us to grow its high-quality crystals *via* melting conditions.

In UV and visible absorption spectra of hybrid crystals, absorption edges were found to be around 450 nm for CNP/CdI_4 and around 400 nm for DAP/CdI_4, respectively. These wavelengths were almost the same as those of the iodide salts.

The crystallographic data of CNP/CdI_4 and DAP/CdI_4 are summarized in Table I. Their ORTEP diagrams in an asymmetric unit are displayed in Figures 2 and 3. The fractional atomic coordinates of these crystals are listed in Tables II and III. Tables IV and V list their bond lengths and bond angles.

As mentioned in the Introduction, hybrid crystals composed of primary ammonium halide and divalent metal halide (2 : 1) are often obtained in a layered perovskite structure, in which halogen anions form corner-sharing octahedra centered by divalent metal atoms. In this structure, the organic portion forms tail-to-tail bilayers or interdigitated monolayers, sandwiched with inorganic sheets. Although CNP/CdI_4 forms a layered structure in crystals, as seen from Figure 4, the inorganic part is composed not of typical octahedral structures but of tetrahedral $[CdI_4]^{2-}$ structures. This structural change can be considered from the area per divalent metal in the layer plane. Figure 5 displays schematic

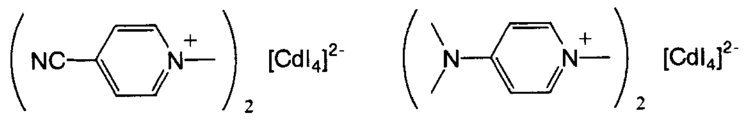

CNP/CdI$_4$ **DAP/CdI$_4$**

FIGURE 1 Chemical structures of CNP/CdI$_4$ and DAP/CdI$_4$.

TABLE I Crystallographic data of CNP/CdI$_4$ and DAP/CdI$_4$

Abbreviation	CNP/CdI$_4$	DAP/CdI$_4$
Formula	$C_{14}H_{14}N_4I_4Cd$	$C_{16}H_{26}N_4I_4Cd$
Formula Weight	858.30	894.50
Crystal Color	Yellow	Pale Yellow
Crystal Size/mm^3	0.3 × 0.3 × 0.2	0.4 × 0.35 × 0.3
Crystal System	Triclinic	Monoclinic
Space Group	$P\bar{1}$	Cc
a/Å	14.833(7)	13.988(8)
b/Å	11.103(4)	14.041(9)
c/Å	7.843(8)	14.877(7)
α/°	110.50(6)	
β/°	74.67(5)	116.02(4)
γ/°	112.61(3)	
V/Å^3	1108.0(1)	2625.9(2)
Z	2	4
D_{calc}/ Mg·m^{-3}	2.572	2.262
μ(MoKα)/mm^{-1}	65.022	54.918
No. of total reflections	5640	3384
No.of unique reflections	4884	3004
No. of reflections with $I < 3\sigma(I)$	4198	2773
R	0.055	0.040
R_w	0.061	0.039

drawings for three types of $[MX_4]^{2-}$, where M and X are a divalent metal and a halide, respectively. The area of the smallest cross-section of a counter ammonium should be smaller than that of a dark rectangle (S) indicated in Figure 5 and the area of a counter ammonium projected perpendicular to the layer plane should coincide to S. The typical octahedral layered perovskite structure is shown in Figure 5(a). The area S for the octahedral structure is calculated using a Cd–I bond length of 3.0 Å to be about 36 Å^2. However, when S exceeds 36 Å^2 due to the bulkiness of counter ammoniums, the octahedral structure is deformed by releasing two halides among four sheared halides in the pure octahedral structure to give a distorted octahedral structure as shown in Figure 5(b). This type of structure has been reported by Azumi *et al.* in a similar hybrid system, *i.e.*, the *p*-nitroanilinium-CdCl$_2$ system [23]. When S increases much more, the distance between divalent metal becomes naturally longer, and finally the interaction from the adjacent metal coordination species can be ignored to form a tetrahedral $[CdI_4]^{2-}$ structure as shown in Figure 5(c). This is the case of CNP/CdI$_4$, whose S is about 56 Å^2.

For DAP/CdI$_4$, the anion part was also found to be a tetrahedral structure. However, $[CdI_4]^{2}$ anions in this crystal do not have a layered structure like CNP/CdI$_4$ but form a one-dimensional column structure along the c axis as shown in Figure 6. Since the tetrahedral $[CdI_4]^{2-}$ structure has more degrees of freedom in its orientation and alignment than the octahedral

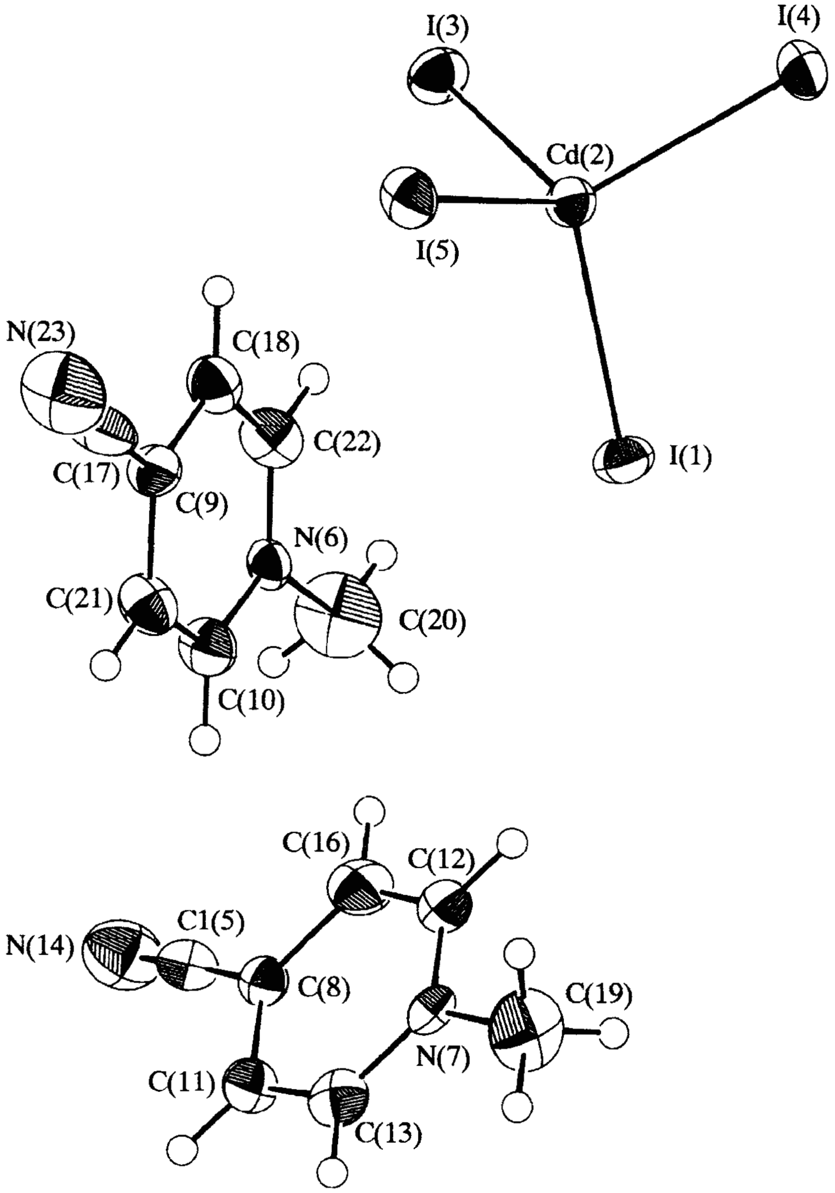

FIGURE 2 ORTEP diagram of a CNP/CdI_4 asymmetric unit.

one, both layered and column structures seemed to be possible. This structural difference seemed to cause a non-centrosymmetric structure in the DAP/CdI_4 crystal.

The DAP/CdI_4 crystal belongs to a non-centrosymmetric space group. This non-centrosymmetry in molecular arrangement was also confirmed by SHG from the powder of DAP/CdI_4. Thus, we estimated the *d* values using the oriented gas model [24]. In the DAP/CdI_4 crystal, the polar axis is the *a* axis. The π-conjugated planes of pyridinium rings in the crystal are almost parallel to the (001) plane. The large *d* components are expected for the case

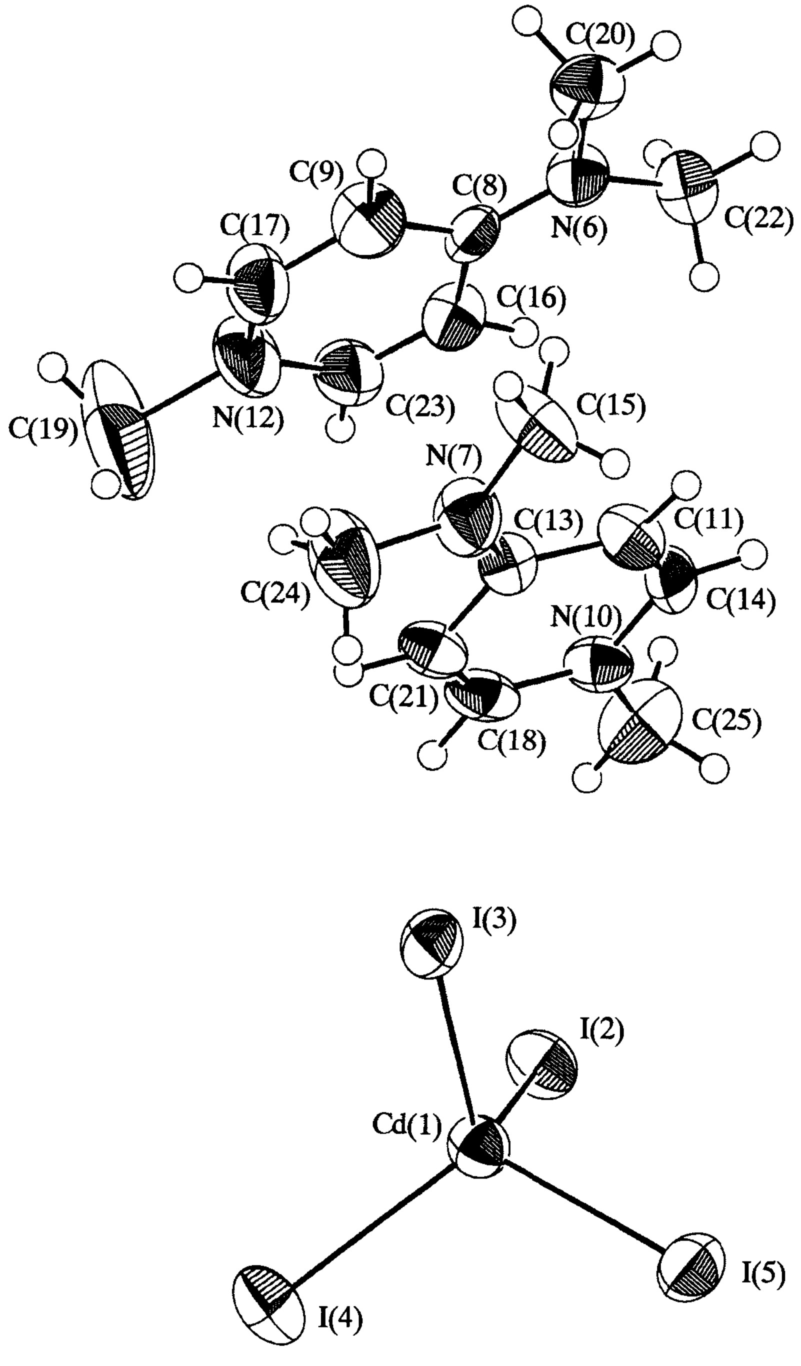

FIGURE 3 ORTEP diagram of a DAP/CdI$_4$ asymmetric unit.

where the input laser is irradiated perpendicular to the plane, shown in Figure 7. There are two series of pyridinium cations with respect to the crystallographic *a* axis, and the angles between the charge transfer (CT) axis of the pyridinium cation and the crystallographic *a* axis are 23.0°

TABLE II Fractional atomic coordinates and equivalent isotropic displacement parameters with e.s.d's in parentheses of CNP/CdI_4

Atom	*x/a*	*y/b*	*z/c*	*U(iso)*
I(1)	0.90940(7)	0.25490(9)	1.0015(1)	0.0409(5)
Cd(2)	0.74990(7)	0.2501(1)	0.8775(1)	0.0318(5)
I(3)	0.80460(7)	0.47970(9)	0.7562(1)	0.0421(5)
I(4)	0.59060(7)	0.24490(9)	1.1559(1)	0.0393(5)
I(5)	0.69540(7)	0.02020(9)	0.5811(1)	0.0394(5)
N(6)	1.1101(7)	0.312(1)	0.572(1)	0.028(5)
N(7)	1.3896(7)	0.190(1)	0.8720(1)	0.029(5)
C(8)	1.5068(9)	0.390(1)	0.714(2)	0.033(7)
C(9)	0.9937(9)	0.112(1)	0.331(2)	0.034(7)
C(10)	1.138(1)	0.206(1)	0.471(2)	0.038(7)
C(11)	1.532(1)	0.278(1)	0.678(2)	0.038(7)
C(12)	1.362(1)	0.294(1)	0.905(2)	0.038(7)
C(13)	1.472(1)	0.180(1)	0.763(2)	0.036(7)
N(14)	1.620(1)	0.597(1)	0.594(2)	0.064(9)
C(15)	1.567(1)	0.502(2)	0.649(2)	0.050(9)
C(16)	1.418(1)	0.399(2)	0.826(2)	0.045(8)
C(17)	0.931(1)	−0.005(2)	0.212(2)	0.050(9)
C(18)	0.967(1)	0.223(1)	0.432(2)	0.039(7)
C(19)	1.328(2)	0.082(2)	0.964(3)	0.06(1)
C(20)	1.170(1)	0.417(2)	0.711(3)	0.06(1)
C(21)	1.081(1)	0.099(1)	0.346(2)	0.038(7)
C(22)	1.028(1)	0.322(1)	0.553(2)	0.040(7)
N(23)	0.878(1)	−0.097(1)	0.122(2)	0.068(9)
H(20A)	1.150	0.495	0.784	0.7(5)
H(20B)	1.234	0.450	0.646	0.1(1)
H(20C)	1.173	0.374	0.795	1.2(3)
H(19A)	1.349	0.005	0.940	0.4(2)
H(19B)	1.264	0.048	0.928	0.1(1)
H(19C)	1.323	0.124	1.095	0.4(3)
H(12)	1.301	0.299	0.984	0.02(3)
H(16)	1.398	0.476	0.850	0.5(4)
H(11)	1.591	0.268	0.597	0.04(4)
H(13)	1.490	0.101	0.742	0.9(2)
H(10)	1.199	0.201	0.484	0.03(3)
H(21)	1.100	0.021	0.274	0.4(2)
H(18)	0.907	0.230	0.421	0.01(3)
H(22)	1.011	0.402	0.626	0.18(8)

and 65.9°, respectively (Fig. 7). Since the largest β component, *i.e.*, β_{zzz}, is parallel to the CT axis, the d values of the crystal are expressed by the following equations:

$$d_{IJK} = N \cdot f_I(\omega_3) \cdot f_J(\omega_1) \cdot f_K(\omega_2) \cdot b_{IJK}. \qquad (1)$$

where

$$b_{IJK} = \frac{1}{N_g}\left(\sum_{s=1}^{N_g} \cos\theta_{Iz}^{(s)} \cdot \cos\theta_{Jz}^{(s)} \cdot \cos\theta_{Kz}^{(s)}\right)\beta_{zzz}. \qquad (2)$$

In these equations, N is the number of molecules per unit volume in the crystal, which is related to the unit cell volume V and the number of equivalent sites N_g as $N = N_g/V$. The angle between the optical axis I and molecular CT axis z is expressed as $\theta_{Iz}^{(s)}$. Factor $f_I(\omega_3)$ is for the correction on the local field along the I axis at ω_3 frequency, and is expressed as $f_I(\omega_3) = (n_I^2(\omega_3) + 2)/3$ using refractive index $n_I(\omega_3)$ along the I axis at ω_3.

When the optical axes X and Y are set parallel to the crystallographic a and b axes, respectively,

TABLE III Fractional atomic coordinates and equivalent isotropic displacement parameters with e.s.d's in parentheses of DAP/CdI_4

Atom	*x/a*	*y/b*	*z/c*	*U(iso)*
Cd(1)	1.1089(1)	0.53480(9)	0.6851(1)	0.0492(8)
I(2)	1.07900	0.67670(8)	0.54300	0.0577(8)
I(3)	0.9527(1)	0.39410(8)	0.6116(1)	0.0608(8)
I(4)	1.3079(1)	0.45120(9)	0.7468(1)	0.0658(8)
I(5)	1.0827(1)	0.62230(9)	0.8412(1)	0.0623(8)
N(6)	0.421(1)	0.4816(9)	0.030(1)	0.050(9)
N(7)	0.6570(1)	0.373(1)	0.317(1)	0.07(1)
C(8)	0.511(1)	0.447(1)	0.038(1)	0.042(9)
C(9)	0.527(2)	0.347(1)	0.044(2)	0.07(1)
N(10)	0.777(1)	0.6346(9)	0.299(1)	0.046(8)
C(11)	0.636(1)	0.542(1)	0.297(1)	0.05(1)
N(12)	0.700(1)	0.369(1)	0.056(1)	0.08(1)
C(13)	0.696(1)	0.456(1)	0.311(1)	0.04(1)
C(14)	0.673(2)	0.625(1)	0.287(2)	0.05(1)
C(15)	0.545(2)	0.356(2)	0.301(2)	0.08(2)
C(16)	0.599(1)	0.503(1)	0.044(2)	0.05(1)
C(17)	0.624(2)	0.313(1)	0.052(2)	0.07(1)
C(18)	0.836(1)	0.554(1)	0.317(1)	0.05(1)
C(19)	0.810(2)	0.323(2)	0.071(3)	0.18(3)
C(20)	0.334(2)	0.422(1)	0.015(1)	0.06(1)
C(21)	0.802(1)	0.466(1)	0.322(1)	0.05(1)
C(22)	0.403(2)	0.585(1)	0.023(2)	0.06(1)
C(23)	0.687(2)	0.467(1)	0.052(2)	0.06(1)
C(24)	0.725(2)	0.286(1)	0.344(2)	0.10(2)
C(25)	0.826(2)	0.728(1)	0.293(2)	0.08(2)
H(20A)	0.268	0.449	0.011	0.05(5)
H(20B)	0.360	0.380	0.072	0.04(4)
H(20C)	0.316	0.386	−0.044	0.14(6)
H(22A)	0.338	0.611	0.018	0.05(6)
H(22B)	0.409	0.604	−0.036	0.05(3)
H(22C)	0.460	0.614	0.080	0.00(8)
H(9)	0.470	0.304	0.037	0.01(3)
H(16)	0.593	0.571	0.045	0.01(3)
H(17)	0.635	0.245	0.060	0.2(1)
H(23)	0.744	0.508	0.056	0.3(1)
H(19A)	0.868	0.361	0.072	0.7(2)
H(19B)	0.794	0.278	0.017	0.2(1)
H(19C)	0.836	0.289	0.133	0.2(1)
H(15A)	0.515	0.296	0.303	0.4(2)
H(15B)	0.501	0.381	0.235	0.05(7)
H(15C)	0.536	0.395	0.350	1.5(2)
H(24A)	0.694	0.225	0.346	0.7(2)
H(24B)	0.784	0.297	0.408	0.3(1)
H(24C)	0.751	0.282	0.294	0.03(6)
H(21)	0.847	0.412	0.331	0.08(7)
H(11)	0.566	0.538	0.294	0.02(3)
H(14)	0.629	0.680	0.273	0.04(4)
H(18)	0.909	0.561	0.327	0.01(2)
H(25A)	0.897	0.733	0.300	0.3(2)
H(25B)	0.822	0.766	0.346	0.07(8)
H(25C)	0.780	0.756	0.230	0.3(1)

TABLE IV Bond lengths and bond angles of CNP/CdI$_4$ in crystals

Bond length/Å			
I(1)—Cd(2)	2.770(2)	Cd(2)—I(3)	2.786(2)
Cd(2)—I(4)	2.764(2)	Cd(2)—I(5)	2.798(2)
N(6)—C(10)	1.31(2)	N(6)—C(20)	1.47(2)
N(6)—C(22)	1.32(2)	N(7)—C(12)	1.30(2)
N(7)—C(13)	1.31(2)	N(7)—C(19)	1.49(3)
C(8)—C(11)	1.35(2)	C(8)—C(15)	1.39(2)
C(8)—C(16)	1.40(2)	C(9)—C(17)	1.45(2)
C(9)—C(18)	1.35(2)	C(9)—C(21)	1.40(2)
C(10)—C(21)	1.39(2)	C(11)—C(13)	1.37(2)
C(12)—C(16)	1.38(2)	N(14)—C(15)	1.20(3)
C(17)—N(23)	1.16(3)	C(18)—C(22)	1.38(2)
Bond angle/degree			
I(1)—Cd(2)—I(3)	108.4(1)	I(1)—Cd(2)—I(4)	110.4(1)
I(1)—Cd(2)—I(5)	110.6(1)	I(3)—Cd(2)—I(4)	110.7(1)
I(3)—Cd(2)—I(5)	108.2(1)	I(4)—Cd(2)—I(5)	108.5(1)
C(10)—N(6)—C(20)	119(1)	C(10)—N(6)—C(22)	121(1)
C(20)—N(6)—C(22)	120(1)	C(12)—N(7)—C(13)	121.3(1)
C(12)—N(7)—C(19)	119(1)	C(13)—N(7)—C(19)	120(1)
C(11)—C(8)—C(15)	123(1)	C(11)—C(8)—C(16)	119(1)
C(15)—C(8)—C(16)	117(1)	C(17)—C(9)—C(18)	123(1)
C(17)—C(9)—C(21)	116(1)	C(18)—C(9)—C(21)	121(1)
N(6)—C(10)—C(21)	122(1)	C(8)—C(11)—C(13)	118(1)
N(7)—C(12)—C(16)	120(1)	N(7)—C(13)—C(11)	122(1)
C(8)—C(15)—N(14)	178(2)	C(8)—C(16)—C(12)	119(1)
C(9)—C(17)—N(23)	177(2)	C(9)—C(18)—C(22)	117(1)
C(9)—C(21)—C(10)	117(1)	N(6)—C(22)—C(18)	122(1)

TABLE V Bond lengths and bond angles of DAP/CdI$_4$ in crystals

Bond length/Å			
Cd(1)—I(2)	2.800(2)	Cd(1)—I(3)	2.789(3)
Cd(1)—I(4)	2.780(3)	Cd(1)—I(5)	2.790(3)
N(6)—C(8)	1.31(3)	N(6)—C(20)	1.41(3)
N(6)—C(22)	1.47(3)	N(7)—C(13)	1.31(3)
N(7)—C(15)	1.48(3)	N(7)—C(24)	1.49(3)
C(8)—C(9)	1.41(3)	C(8)—C(16)	1.43(3)
C(9)—C(17)	1.39(3)	N(10)—C(14)	1.39(3)
N(10)—C(18)	1.36(3)	N(10)—C(25)	1.51(3)
C(11)—C(13)	1.43(3)	C(11)—C(14)	1.30(3)
N(12)—C(17)	1.32(3)	N(12)—C(19)	1.59(4)
N(12)—C(23)	1.38(3)	C(13)—C(21)	1.42(3)
C(16)—C(23)	1.29(3)	C(18)—C(21)	1.34(3)
Bond angle/degree			
I(2)—Cd(1)—I(3)	112.1(1)	I(2)—Cd(1)—I(4)	110.3(1)
I(2)—Cd(1)—I(5)	106.5(1)	I(3)—Cd(1)—I(4)	109.2(1)
I(3)—Cd(1)—I(5)	105.8(1)	I(4)—Cd(1)—I(5)	112.9(1)
C(8)—N(6)—C(20)	122(1)	C(8)—N(6)—C(22)	121(1)
C(20)—N(6)—C(22)	117(2)	C(13)—N(7)—C(15)	122(2)
C(13)—N(7)—C(24)	121(2)	C(15)—N(7)—C(24)	115(2)
N(6)—C(8)—C(9)	120(2)	N(6)—C(8)—C(16)	124(1)
C(9)—C(8)—C(16)	116(2)	C(8)—C(9)—C(17)	118(2)

TABLE V (Continued)

C(14)—N(10)—C(18)	117(2)	C(14)—N(10)—C(25)	124(2)
C(18)—N(10)—C(25)	119(2)	C(13)—C(11)—C(14)	122(2)
C(17)—N(12)—C(19)	118(2)	C(17)—N(12)—C(23)	120(2)
C(19)—N(12)—C(23)	121(2)	N(7)—C(13)—C(11)	122(2)
N(7)—C(13)—C(21)	122(2)	C(11)—C(13)—C(21)	117(2)
N(10)—C(14)—C(11)	121(2)	C(8)—C(16)—C(23)	123(2)
C(9)—C(17)—N(12)	123(2)	N(10)—C(18)—C(21)	125(2)
C(13)—C(21)—C(18)	118(2)	N(12)—C(23)—C(16)	120(2)

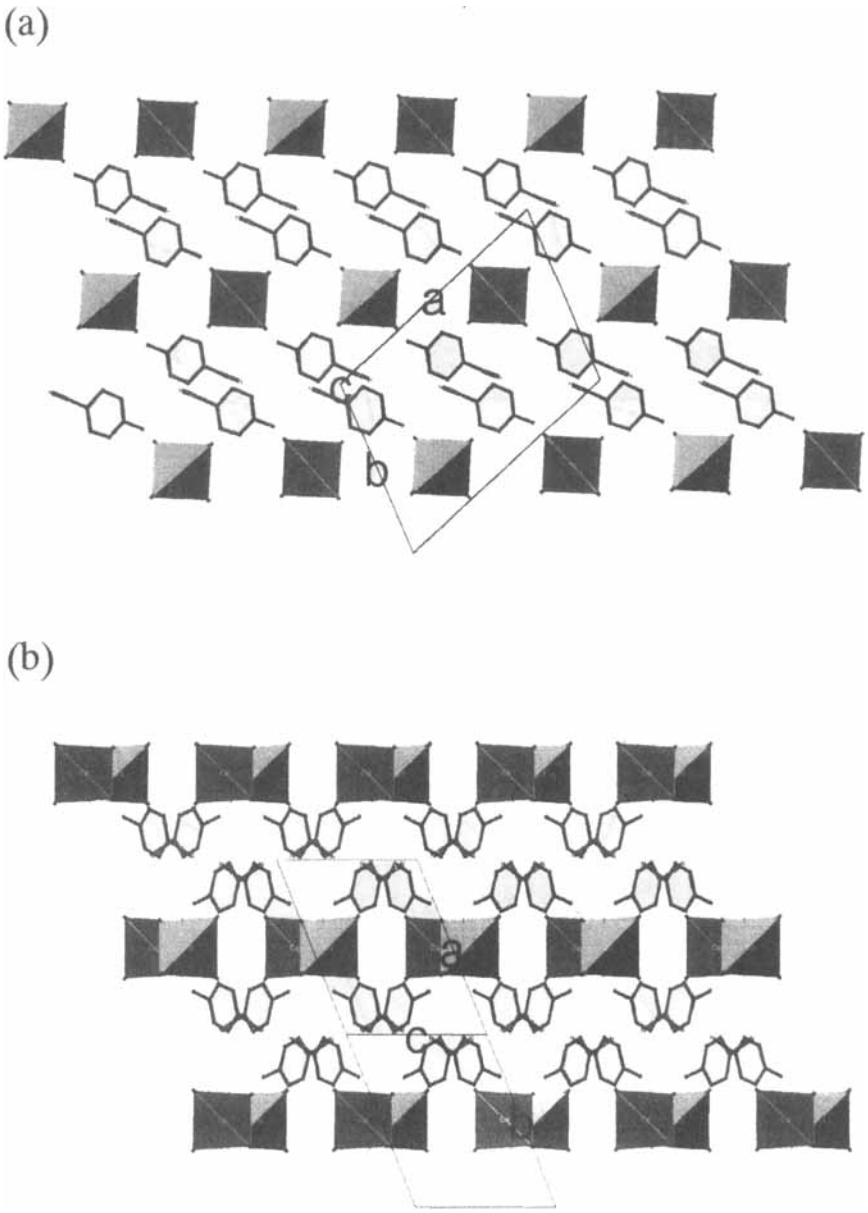

FIGURE 4 Molecular packing of CNP/CdI$_4$: views along the [001] direction (a) and the [110] direction (b). [CdI$_4$]$^{2-}$ anions are displayed using tetrahedra.

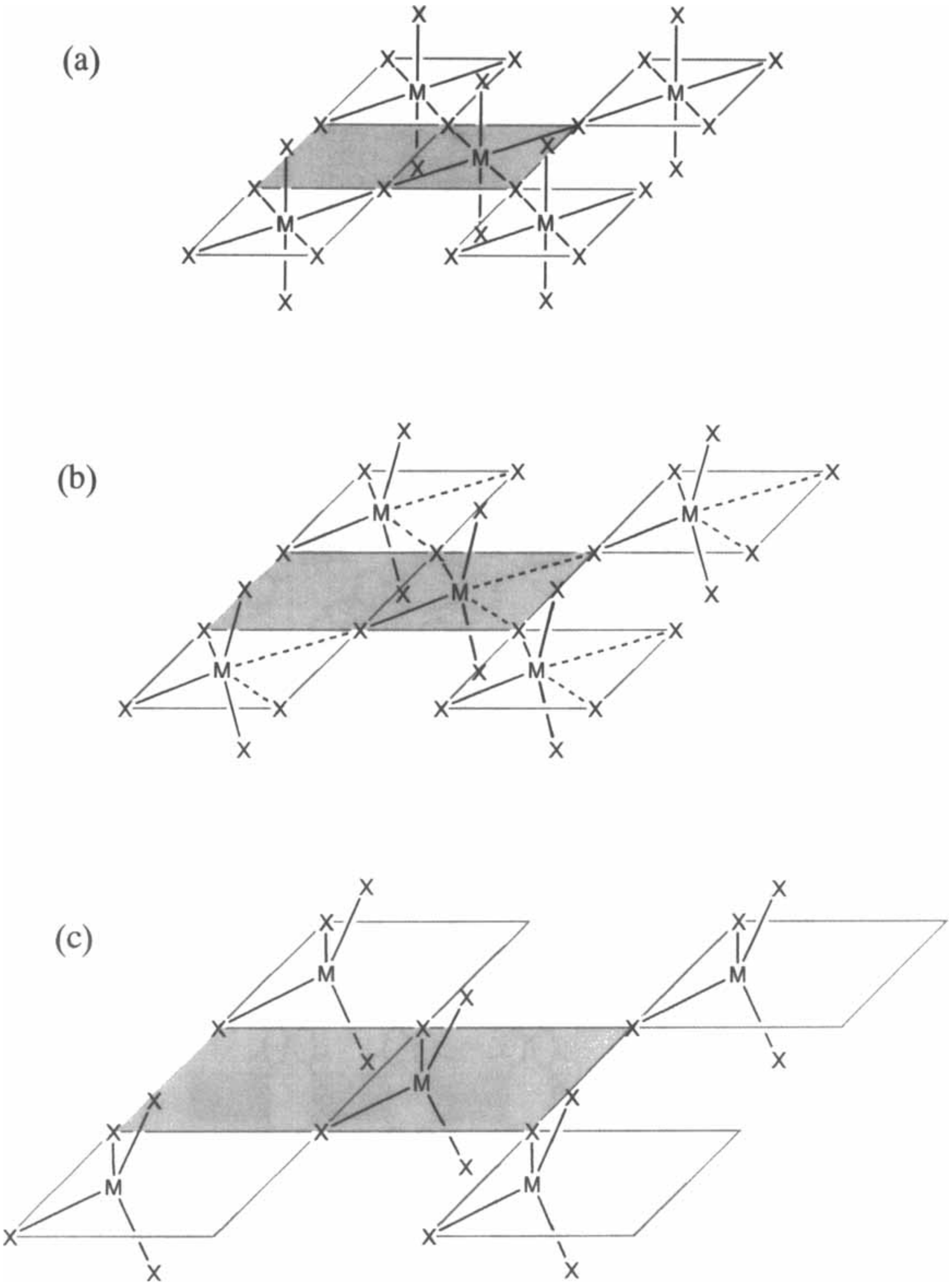

FIGURE 5 Schematic structural diagrams for hybrid crystals composed of ammonium halide and divalent metal halide: (a) Octahedral structure, (b) distorted octahedral structure and (c) tetrahedral structure. In these figures, only the inorganic parts are drawn, and M and X represent metal and halide atoms, respectively.

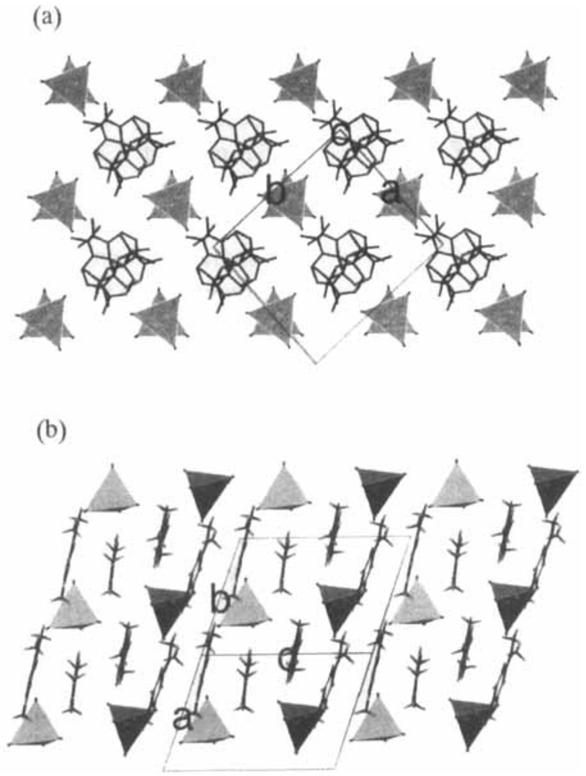

FIGURE 6 Molecular packing of DAP/CdI$_4$: views along the [001] direction (a) and the [110] direction (b). $[\mathrm{CdI_4}]^{2-}$ anions are displayed using tetrahedra.

as shown in Figure 7, the d_{XXX} and d_{XYY} can be expressed as

$$d_{XXX} = N \cdot f_1(2\omega) \cdot f_1^2(\omega) \cdot \beta_{zzz}(\cos^3 23.0^\circ + \cos^3 65.9^\circ) \tag{3}$$

and

$$d_{XYY} = N \cdot f_1(2\omega) \cdot f_2^2(\omega) \cdot \beta_{zzz}(\cos 23.0^\circ \sin^2 23.0^\circ + \cos 65.9^\circ \sin^2 65.9^\circ). \tag{4}$$

The β_{zzz} value used was 7.3×10^{-30} esu which was calculated using the MOPAC PM3 method, and N is 1.53×10^{21} molecules/cm^3. Since the refractive index of the DAP/CdI$_4$ crystal could not be evaluated, we simply assumed it to have the same values as the 2-methyl-4-nitroaniline (MNA) crystal, which is well known as a second-order NLO compound [25,26]. As the result, we obtained 28 pm/V for d_{XXX} and 12 pm/V for d_{XYY} as the fundamental beam at 1064 nm was assumed. The d values of MNA were also calculated in a similar way using $\theta = 21^\circ$, $N = 5.73 \times 10^{21}$ molecules/cm^3 and $\beta_{zzz} = 6.3 \times 10^{-30}$ esu to obtain 86 pm/V for d_{11} and 9.5 pm/V for d_{12}. Thus, the d values of DAP/CdI$_4$ were predicted to be one-third in the diagonal component and four-thirds in the off-diagonal component of those of MNA. Although the maximum d value of DAP/CdI$_4$ is estimated to be smaller than that of MNA, the absorption cutoff wavelength of the DAP/CdI$_4$ is about 100 nm shorter than that of MNA, resulting in a wider range of input lasers.

In conclusion, we prepared two pyridinium-CdI$_2$ hybrid crystals, *i.e.*, CNP/CdI$_4$ and

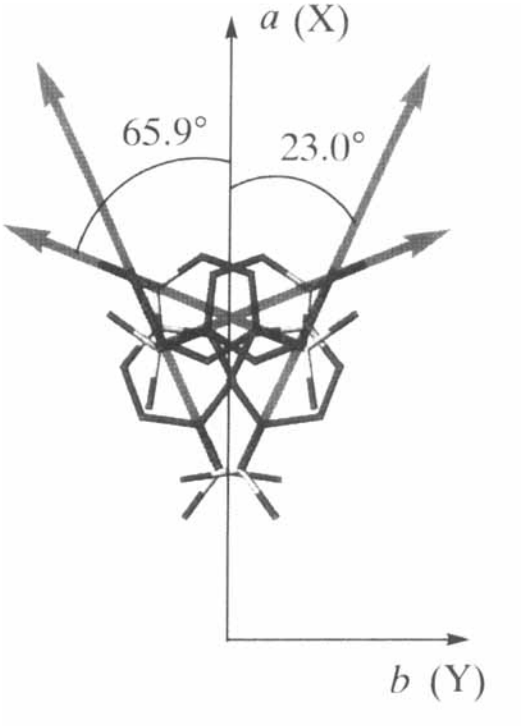

FIGURE 7 Orientation of DAP cation in the hybrid crystal with respect to crystallographic axes *a* and *b* and optical axes *X* and *Y*. The angles between the cationic CT axis and the crystallographic polar *a* axis parallel to the optical *X* axis are shown.

DAP/CdI_4, and their crystal structures were investigated. As the anionic species, tetrahedral $[CdI_4]^{2-}$ structures were confirmed for two crystals. CNP/CdI_4 was found to form a centrosymmetric layered structure, while DAP/CdI_4 does not have a layered structure but forms a one-dimensional column structure for $[CdI_4]^{2-}$ anions. As a result, DAP/CdI_4 forms non-centrosymmetric crystals. The *d* values of the DAP/CdI_4 crystal were estimated using the oriented gas model. Irrespective of the absorption cutoff wavelength of DAP/CdI_4 being about 100 nm shorter than that of the MNA crystal, *d* values were expected to reach one-third in the diagonal component and four-thirds in the off-diagonal component of those of MNA. And this crystal has one of the merits of crystal growth, to use melt-growth techniques.

EXPERIMENTAL

Typical procedures to synthesize pyridinium iodide-CdI_2 hybrid crystals are as follows: 5 mmol of CNP iodide or DAP iodide was dissolved in 50 ml of ethanol, and 2.5 mmol of cadmium iodide was dissolved in 50 ml of ethanol. When the two solutions were mixed, precipitation immediately occurred. Precipitated powder crystals were filtered, washed with ethanol, and dried. The yields were 92% for CNP/CdI_4 and 97% for DAP/CdI_4. Single crystals of hybrid compounds were obtained by the slow-evaporation method: Concentrated acetone solutions of these powder crystals were put in vessels covered with aluminum foil having several pin-holes and they were kept at room temperature for a few weeks to give hybrid single crystals. For X-ray crystallographic analysis, cell parameters and intensity data were derived from measurements on a MacScience MXC18 diffractmeter with graphite-monochromotized MoKα radiation. All calculations were performed using the CRYSTAN program.

References

[1] *Nonlinear Optical Properties of Organic Molecules and Crystals*, Vols. 1 and 2, Chemla, D. S. and Zyss, J. (Eds.), Academic Press, Orland, 1987.

[2] Organic Nonlinear Optical Materials, Kikan Kagaku Sosetsu, 15, *Chem. Soc. Jpn.*, (Eds.), Gakkai Shuppan Center, Tokyo, 1992. [in Japanese].

[3] *Molecular Nonlinear Optics*, Zyss, J. (Ed.), Academic Press, Orland, 1994.

[4] *Optical Nonlinearities in Chemistry*, *Chem. Rev.*, 94, 1, 1994.

[5] Bosshard, Ch., Sutter, K., Prêtre, Ph., Hulliger, J., Flörsheimer, M., Kaatz, P. and Günter, P., *Organic Nonlinear Optical Materials*, *Advances in Nonlinear Optics*, p. 1, Gordon and Breach Publishers, Basel, 1995.

[6] *Nonlinear Optics of Organic Molecules and Polymers*, Nalwa, H. S. and Miyata, S. (Eds.), CRC Press, Boca Raton, 1997.

[7] Japanese patent application 61-192404 (1986); Japanese patent 1716929 (1992).

[8] Nakanishi, H., Matsuda, H., Okada, S. and Kato, M., *Mater. Res. Soc. Int. Mtg. Adv. Mater.*, **1**, Doyama, M., Somiya, S. and Chang, R. P. H. (Eds.), Material Research Society, Pittsburgh, 1989, p. 97.

[9] Mader, S. R., Perry, J. W. and Schaefer, W. P. (1989). *Science*, **245**, 626.

[10] Duan, X.-M., Konami, H., Okada, S., Oikawa, H., Matsuda, H. and Nakanishi, H. (1996). *J. Phys. Chem.*, **100**, 17780.

[11] Marder, S. R., Perry, J. W. and Yakymyshyn, C. P. (1994). *Chem. Mater.*, **6**, 1137.

[12] Knöpfle, G., Schlesser, R., Ducret, R. and Günter, P. (1995). *Nonlinear Opt.*, **9**, 143.

[13] Anwar, Duan, X.-M., Komatsu, K., Okada, S., Matsuda, H., Oikawa, H. and Nakanishi, H. (1997). *Chem. Lett.*, p. 247.

[14] Anwar, Komatsu, K., Okada, S., Oikawa, H., Matsuda, H. and Nakanishi, H. (1999). *Proc. SPIE*, **3796**, 219.

[15] Anwar, Duan, X.-M., Komatsu, K., Okada, S., Oikawa, H., Matsuda, H. and Nakanishi, H. (1999). *Nonlinear Opt.*, **22**, 251.

[16] Anwar, Okada, S., Oikawa, H. and Nakanishi, H. (2000). *Chem. Mater.*, **12**, 1162.

[17] Xu, C.-Q., Kondo, T., Sakakura, H., Kumata, K., Takahashi, Y. and Ito, R. (1991). *Solid State Commun.*, **79**, 245.

[18] Hong, X., Ishihara, T. and Nurmikko, A. V. (1992). *Phys. Rev. B*, **45**, 6961.

[19] Papavassiliou, G. C., Patsis, A. P., Lagouvardos, D. J. and Koutselas, I. B. (1993). *Synth. Met.*, **57**, 3889.

[20] Era, M., Morimoto, S., Tsutsui, T. and Saito, S. (1994). *Appl. Phys. Lett.*, **65**, 676.

[21] Mitzi, D. B., Field, C. A., Harrison, W. T. A. and Guloy, A. M. (1994). *Nature*, **369**, 467.

[22] Found for CNP/CdI$_4$: C, 19.58; H, 1.71; N, 6.44%. Calcd for $C_{14}H_{14}N_4I_4Cd$: C, 19.59; H, 1.64; N, 6.53%. Found for DAP/CdI$_4$: C, 21.42; H, 2.91; N, 6.26%. Calcd for $C_{16}H_{26}N_4I_4Cd$: C, 21.49; H, 2.93; N, 6.26%.

[23] Azumi, R., Honda, K., Goto, M., Akimoto, J., Oosawa, Y., Tachibana, H., Tanaka, M. and Matsumoto, M. (1996). *Mol. Cryst. Liq. Cryst.*, **276**, 237.

[24] Zyss, J. and Ouder, J. L. (1982). *Phys. Rev. A*, **26**, 2028.

[25] Levine, B. F., Bethea, C. G., Thurmond, C. D., Lynch, R. T. and Bernstein, J. L. (1979). *J. Appl. Phys.*, **50**, 2523.

[26] Lipcomp, G. F., Garito, A. F. and Narang, R. S. (1981). *J. Chem. Phys.*, **75**, 1509.